RIGOROUS NUMERICS FOR NONLINEAR DIFFERENTIAL EQUATIONS USING CHEBYSHEV SERIES

JEAN-PHILIPPE LESSARD* AND CHRISTIAN REINHARDT†

Abstract. A computational method based on Chebyshev series to rigorously compute solutions of initial and boundary value problems of analytic nonlinear vector fields is proposed. The idea is to recast solutions as fixed points of an operator defined on a Banach space of rapidly decaying Chebyshev coefficients and to use the so-called radii polynomials to show the existence of a unique fixed point nearby an approximate solution. As applications, solutions of initial value problems in the Lorenz equations and symmetric connecting orbits in the Gray-Scott equation are rigorously computed. The symmetric connecting orbits are obtained by solving a boundary value problem with one of the boundary values in the stable manifold.

Key words. Rigorous numerics, chebyshev series, nonlinear ODEs, boundary value problems, initial value problems, contraction mapping theorem

AMS subject classifications. 34B99, 34A34, 34A12, 42A10, 65L05, 65L10

1. Introduction. In this paper, we propose a rigorous numerical method based on the Chebyshev polynomials to compute solutions of nonlinear differential equations. More explicitly, the field of rigorous numerics develops algorithms that provide approximate solutions to a problem together with precise bounds within which exact solutions are guaranteed to exist in the mathematically rigorous sense. In this context, the main idea of our proposed approach is to expand the solution of a given differential equation using its Chebyshev series, plug the expansion in the equation, obtain an equivalent infinite dimensional problem of the form $f(x) = 0$ to solve in a Banach space of rapidly decaying Chebyshev coefficients and to get the existence, via a fixed point argument, of a genuine solution of $f(x) = 0$ nearby a numerical approximation of a finite dimensional projection of f. The fixed point argument is solved by using the radii polynomials (e.g. see [1]), which provide an efficient way of constructing a set on which the contraction mapping theorem is applicable.

Before proceeding further, it is worth mentioning that a similar approach based on Fourier series is widely used in the field of rigorous numerics to compute solutions of differential equations with periodic profiles. For instance, time periodic solutions of ODEs [2, 3], stationary solutions of PDEs with periodic or Neumann boundary conditions [4, 5, 6, 7], time periodic solutions of delay differential equations [8, 9] and invariant sets of infinite dimensional maps [10] have been successfully computed using Fourier series and rigorous numerics. However, while being a well established tool in the scientific computing literature [12, 15, 19, 20, 21, 22], to the best of our knowledge, this is the first time that a method based on Chebyshev series is presented to rigorously compute solutions of nonlinear differential equations. Since this includes a large class of non-periodic solutions to ODEs (e.g. solutions of initial value problems (IVPs) and boundary value problems (BVPs) with non periodic boundary values), in the realm of the rigorous numerical approach described above, we believe that our proposed approach is a valuable contribution to the field of rigorous numerics. Also,

*Université Laval, Département de Mathématiques et de Statistique, 1045 avenue de la Médecine, Québec, QC, G1V 0A6, Canada. jean-philippe.lessard@mat.ulaval.ca.

†Technische Universität München, Zentrum Mathematik, Boltzmannstrasse 3, 85747 Garching, Germany. reinhard@ma.tum.de. This author was supported by the ENB graduate program *TopMath*.

since Chebyshev series are Fourier series *in disguise* [12], the mathematical machinery developed in the last ten years to prove existence of solutions with periodic profiles can directly be transferred to prove existence of non periodic solutions. To give a few examples, the analytic estimates introduced in [4, 6, 10, 13] and the Banach space of rapidly decaying coefficients used in [3, 4] can be applied here. In addition, let us mention the work [14] where the authors develop an analogue to Taylor models based on interpolation with Chebyshev polynomials. However, it seems that their methods have not yet been applied to rigorously solve nonlinear differential equations. Finally also in [11] Chebyshev interpolation is used in a rigorous numerical algorithm, but in a different context, namely to approximate non polynomial nonlinearities.

In the present work, we focus our attention to analytic vector fields of the form

$$\frac{du}{dt} = \Psi(u), \quad \Psi : \mathbb{R}^n \to \mathbb{R}^n, \tag{1.1}$$

where we aim at computing rigorously solutions of IVPs and BVPs associated to (1.1). Even if we present the method in this context, we strongly believe that a similar approach could be adapted to directly prove existence of solutions of higher order differential equations without rewriting them as a first order equation. We give some more details on this idea in Section 4.

The Chebyshev polynomials are defined by $T_0(t) = 1$, $T_1(t) = t$ and $T_{k+1}(t) = 2tT_k(t) - T_{k-1}(t)$ for $k \geq 1$. They lead to an analogue of the Fourier expansion for non periodic functions on an interval and, as mentioned earlier, they are Fourier series *in disguise*, as $T_k(\cos\theta) = \cos(k\theta)$. The following standard result can be found in [15].

THEOREM 1.1. *Every Lipschitz continuous function $v : [-1, 1] \to \mathbb{R}$ has a unique representation as an absolutely and uniformly convergent series $v(t) = \sum_{k=0}^{\infty} a_k T_k(t)$.*

The following result, which can also be found in [15], shows that the coefficients a_k of the Chebyshev series of an analytic function v decay exponentially fast to zero.

THEOREM 1.2. *Let a function v analytic in $[-1, 1]$ be analytically continuable to the open ρ-ellipse E_ρ for some $\rho > 1$ where it satisfies $|v(z)| \leq M$ for all $z \in E_\rho$ for some M. Then its Chebyshev coefficients satisfy $|a_k| \leq 2M\rho^{-k}$, with $|a_0| \leq M$ in the case $k = 0$.*

The ellipse E_ρ (with foci at ± 1) is defined by fixing $\rho > 1$ and considering the image of the circle with radius ρ in the complex plane $\mathbb{C}$ under the map $z \mapsto \frac{1}{2}(z+z^{-1})$. The following Corollary 1.3 which is a consequence of Theorem 1.1 and Theorem 1.2 plays a fundamental role in the design of our approach.

COROLLARY 1.3. *Assume that $\Psi : \mathbb{R}^n \to \mathbb{R}^n$ is real analytic and let $u : [-1, 1] \to \mathbb{R}^n$ be a solution of (1.1). Then each component u_j of u is real analytic and has a unique representation as an absolutely and uniformly convergent series of the form $u_j(t) = \sum_{k=0}^{\infty} (a_j)_k T_k(t)$. Also, for each $j \in \{1, \ldots, n\}$, the sequence of Chebyshev coefficients $\{(a_j)_k\}_{k\geq 0}$ of u_j decreases to zero faster than any algebraic decay, that is, for any decay rate $s > 1$, there exists a constant $C_j = C_j(s) < \infty$ such that $|(a_j)_k| \leq \frac{C_j}{k^s}$, for $k \geq 1$.*

Consider a Chebyshev expansion of a solution u of the analytic vector field (1.1)

$$u(t) = a_0 + 2\sum_{k\geq 1} a_k T_k(t), \tag{1.2}$$

where $a_k = \big((a_1)_k, (a_2)_k, \cdots, (a_n)_k\big)^T \in \mathbb{R}^n$. Letting $\|a_k\|_\infty = \max_{j=1,\ldots,n}\{|(a_j)_k|\}$

and defining the weights

$$\omega_k^s \stackrel{\text{def}}{=} \begin{cases} 1, & \text{if } k = 0 \\ |k|^s, & \text{if } k \neq 0, \end{cases} \tag{1.3}$$

one has by Corollary 1.3 that for any given $s > 1$

$$\|a\|_s \stackrel{\text{def}}{=} \sup_{k\geq 0}\{\|a_k\|_\infty \omega_k^s\} < \infty. \tag{1.4}$$

The philosophy of our method is therefore to rigorously compute solutions u of an IVP or a BVP associated to (1.1) first by recasting them as solutions of an operator equation

$$F(u) = 0, \tag{1.5}$$

and then to use Chebyshev series to transform (1.5) into an equivalent problem of the form

$$f(x) = 0, \tag{1.6}$$

to solve in a Banach space X^s of algebraically decaying Chebyshev coefficients. We now introduce the operators (1.5) and (1.6), first for IVPs and then for BVPs.

Initial value problems. The first class of problems we address in the present work are initial value problems associated to the vector field (1.1). Integrating (1.1) from -1 to t, one has that finding a solution u with initial condition $u(-1) = p_0 \in \mathbb{R}^n$ is equivalent to finding a solution u of $F(u) = 0$, where the nonlinear operator F is given by

$$F(u)(t) \stackrel{\text{def}}{=} p_0 + \int_{-1}^{t} \Psi(u(s))ds - u(t), \quad t \in [-1, 1]. \tag{1.7}$$

The fact that $t \in [-1, 1]$ is not a restriction since in the autonomous vector field (1.1), a re-scaling of time could be considered. The goal is to develop a rigorous computational method based on Chebyshev series to compute solutions of (1.7). Given the Chebyshev expansion (1.2) of u with $a = (a_k)_{k\geq 0}$ the infinite vector of Chebyshev coefficients, consider the Chebyshev expansion of $\Psi(u)$ given by

$$\Psi(u(t)) = c_0 + 2\sum_{k\geq 1} c_k T_k(t), \tag{1.8}$$

where $c_k = c_k(a) = \big((c_1)_k, (c_2)_k, \cdots, (c_n)_k\big)^T \in \mathbb{R}^n$. In particular, if $\Psi(u)$ is a polynomial vector field, then since Chebyshev polynomials satisfy $T_k(\cos\theta) = \cos(k\theta)$, c_k is given by discrete convolutions involving the coefficients of a. Plugging (1.2) and (1.8) in (1.7), and using the properties $T_k(-1) = (-1)^k$ and $T_k(1) = 1$ for all k, $\int T_0(s)ds = T_1(s)$, $\int T_1(s)ds = (T_2(s) + T_0(s))/4$ and $\int T_k(s)ds = \frac{1}{2}\left(\frac{T_{k+1}(s)}{k+1} - \frac{T_{k-1}(s)}{k-1}\right)$ for $k \geq 2$, one gets that

$$F(u)(t) = \tilde{f}_0 + 2\sum_{k\geq 1} \tilde{f}_k T_k(t),$$

where $\tilde{f}_0 \stackrel{\text{def}}{=} p_0 - a_0 + c_0 - \frac{c_1}{2} - 2\sum_{j\geq 2}\frac{(-1)^j}{j^2-1}c_j$ and $\tilde{f}_k \stackrel{\text{def}}{=} \frac{c_{k-1}-c_{k+1}}{2k} - a_k$, for $k \geq 1$. Denote $x = a$ and define $f(x) = (f_k(x))_{k\geq 0}$ component-wise by

$$f_k(x) \stackrel{\text{def}}{=} \begin{cases} p_0 - a_0 - 2\displaystyle\sum_{j=1}^{\infty}(-1)^j a_j, & k = 0, \\ 2ka_k + c_{k+1} - c_{k-1}, & k \geq 1. \end{cases} \tag{1.9}$$

f given by (1.9) is called the *IVP-operator* and finding a solution u of (1.7) is equivalent to finding a zero of the IVP-operator. To see this, note that $f_k = -2k\tilde{f}_k$ for $k \geq 1$ and that if $2ka_k = c_{k-1} - c_{k+1}$ for all $k \geq 1$ we have that

$$p_0 - a_0 + c_0 - \frac{c_1}{2} - 2\sum_{j=2}^{\infty}\frac{(-1)^j}{j^2-1}c_j = p_0 - a_0 - 2\sum_{j=1}^{\infty}(-1)^j a_j. \tag{1.10}$$

Boundary value problems. A second class of problems that we address in the present work are boundary value problems associated to the vector field (1.1), that is solutions u satisfying the differential equations (1.1) in $[-1, 1]$ while satisfying the boundary condition

$$\mathcal{G}(u(-1), u(1)) = 0, \tag{1.11}$$

where $\mathcal{G} : \mathbb{R}^{2n} \to \mathbb{R}^p$ is an affine map, with p the *number* of boundary conditions. Letting $p_1 = u(1)$, integrating the vector field (1.1) from t to 1 and appending the boundary condition (1.11) results in the integral operator defined by

$$F(\theta, u)(t) \stackrel{\text{def}}{=} \begin{pmatrix} \mathcal{G}(u(-1), u(1)) \\ u(t) + \displaystyle\int_t^1 \Psi(u(s))ds - p_1 \end{pmatrix}, \tag{1.12}$$

where $\mathcal{G}(u(-1), u(1))$ and/or p_1 depend on a parameter $\theta \in \mathbb{R}^p$. For a concrete example for how the map $\mathcal{G}$ is chosen we refer the reader to equation (3.11). Denote by $x = (\theta, a)$ the infinite dimensional vector of unknowns. Following the same approach as the one used to derive the IVP-operator, we plug (1.2) and (1.8) in (1.12), use standard properties of the Chebyshev polynomials and then we define the operator $f(x) = (f_k(x))_{k\geq -1}$ given component-wise by

$$f_k(x) = \begin{cases} \eta(\theta, a), & k = -1, \\ a_0 + 2\displaystyle\sum_{j=1}^{\infty} a_j - p_1 & k = 0, \\ 2ka_k + c_{k+1} - c_{k-1}, & k \geq 1, \end{cases} \tag{1.13}$$

where $\eta \in \mathbb{R}^p$ is a function of $a = (a_k)_{k\geq 0}$ and possibly of θ that represents the boundary condition (1.11) expressed using the Chebyshev expansion of u. We call the operator $f(x) = (f_k(x))_{k\geq -1}$ given by (1.13) the *BVP-operator*. Hence, using a similar observation to (1.10), finding a solution u of the boundary value problem (1.12) is equivalent to finding a zero of the BVP-operator.

Let us introduce the notation $x = (x_k)_{k\geq k_0}$ and $f = (f_k)_{k\geq k_0}$, with $k_0 \in \{-1, 0\}$. If x is the vector of unknowns of the IVP-operator (1.9), then $k_0 = 0$ and $x = (x_k)_{k\geq k_0}$,

with $x_k = a_k \in \mathbb{R}^n$ for $k \geq 0$. If x is the vector of unknown of the BVP-operator (1.13), then $k_0 = -1$ and $x = (x_k)_{k\geq k_0}$, with $x_{-1} = \theta \in \mathbb{R}^p$ and $x_k = a_k \in \mathbb{R}^n$ for $k \geq 0$. Similarly, if f is the IVP-operator (1.9), then $k_0 = 0$ and if f is the BVP-operator (1.13), then $k_0 = -1$ and $f = (f_k)_{k\geq k_0}$, with $f_{-1} = \eta \in \mathbb{R}^p$.

Given $\theta \in \mathbb{R}^p$, let $\|\theta\|_\infty = \max\{|\theta_1|, |\theta_2|, \ldots, |\theta_p|\}$. Recall the weights (1.3). As a consequence of Corollary 1.3, we define the IVP-operator and the BVP-operator on the Banach space of decaying Chebyshev coefficients given by

$$X^s = \{x = (x_k)_{k\geq k_0} : \|x\|_s \stackrel{\text{def}}{=} \sup_{k\geq k_0} \{\|x_k\|_\infty \omega_k^s\} < \infty\}, \tag{1.14}$$

with $k_0 = 0$ in case of the IVP-operator and with $k_0 = -1$ in case of the BVP-operator. The rest of the paper aims at introducing the rigorous method to prove existence of solutions of $f(x) = 0$ within X^s using the notion of the radii polynomials.

The paper is organized as follows. In Section 2, we introduce the rigorous computational method to prove existence of solutions of $f(x) = 0$ within X^s, where f is either the IVP-operator (1.9) or the BVP-operator (1.13). In Section 3, we present some applications. In Section 3.1, rigorous computations of IVPs in the Lorenz equations are introduced while in Section 3.2, we compute symmetric connecting orbits for the Gray-Scott equation. Note that the symmetric connecting orbits are obtained by computing solutions of a BVP with one of the boundary values in the stable manifold. We conclude the paper in Section 4 by presenting some possible extensions and improvements.

2. Rigorous computations. In this section, we introduce the rigorous computational method to compute $x \in X^s$ that are solutions of $f(x) = 0$, where the operator f is either the IVP-operator (1.9) or the BVP-operator (1.13). Let us formalize the definition of the operator f on X^s.

LEMMA 2.1. *Consider the Banach space X^s with $s > 1$, the vector field* (1.1)*, let $x = (x_k)_{k\geq k_0} \in X^s$ and define $u(t) = a_0 + 2\sum_{k\geq 1} a_k T_k(t)$, where $a_k = x_k$ for $k \geq 0$. Assume that the coefficients $(c_k)_{k\geq 0}$ of the Chebyshev series of $\Psi(u)$ given by* (1.8) *satisfy*

$$\|c\|_s = \sup_{k\geq 0}\{\|c_k\|_\infty \omega_k^s\} < \infty. \tag{2.1}$$

Consider f either the IVP-operator (1.9) *or the BVP-operator* (1.13)*. Then, $f : X^s \to X^{s-1}$. Also, if $x \in X^s$ is a solution of $f(x) = 0$, then $x \in X^{s_0}$ for any $s_0 > 1$. Finally, $u(t) = a_0 + 2\sum_{k\geq 1} a_k T_k(t)$ is a solution of $F = 0$ where F is the integral operator* (1.7) *(respectively* (1.12)*) if and only if $x = (x_k)_{k\geq k_0} \in X^s$ solves $f(x) = 0$ where f is the IVP-operator* (1.9) *(respectively the BVP-operator* (1.13)*).*

Before presenting the proof of Lemma 2.1, it is important to remark that the hypothesis (2.1) is met for all polynomial vector fields, since for any $s > 1$, $\Omega^s \stackrel{\text{def}}{=} \{a = (a_k)_{k\in\mathbb{N}} : a_k \in \mathbb{R},\ \|a\|_s < \infty\}$ is an algebra under the discrete convolution. More precisely for any $a, b \in \Omega^s$, there exists a constant $\alpha = \alpha(a, b) < \infty$ such that $|(a * b)_k| = |\sum_{\substack{k_1+k_2=k \\ k_i\in\mathbb{Z}}} a_{|k_1|} b_{|k_2|}| \leq \frac{\alpha}{\omega_k^s}$ (e.g. see [4] for the case $s \geq 2$ and see [16] for the case $s \in (1, 2)$ for rather sharp values for α). This implies that $a * b \in \Omega^s$, and hence that $(\Omega^s, *)$ is an algebra. For ease of notation we will henceforth omit the $*$.

Proof. (of Lemma 2.1) Consider $x = (x_k)_{k\geq k_0} \in X^s$ and define $u(t) = a_0 + 2\sum_{k\geq 1} a_k T_k(t)$, with $a_k = x_k$ for $k \geq 0$. In case $k_0 = -1$, one clearly has that $\|f_{k_0}(x)\|_\infty = \|\eta(x)\|_\infty < \infty$. As $\|a\|_s < \infty$ is equivalent to $\|a_k\|_\infty \leq \frac{\|a\|_s}{\omega_k^s}$, it follows,

since $s > 1$, that $\| \sum_{j=1}^{\infty} (-1)^k a_k \|_\infty \leq \sum_{j=1}^{\infty} \frac{1}{j^s} < \infty$. That implies that $\|f_0(x)\|_\infty < \infty$. Now, there exists a constant $\alpha_1 < \infty$ such that $\|f_k(x)\|_\infty = \|2ka_k + c_{k+1} - c_{k-1}\|_\infty \leq \frac{2\|a\|_s}{\omega_k^{s-1}} + \frac{\|c\|_s}{\omega_{k+1}^s} + \frac{\|c\|_s}{\omega_{k-1}^s} \leq \frac{\alpha_1}{\omega_k^{s-1}}$ for all $k \geq 1$. Thus $\|f(x)\|_{s-1} < \infty$ and therefore $f(x) \in X^{s-1}$.

Assume now that $x \in X^s$ is a solution of $f(x) = 0$. Hence, for any $k \geq 1$, $f_k(x) = 2ka_k + c_{k+1} - c_{k-1} = 0$ which implies that $a_k = -\frac{1}{2k}(c_{k+1} - c_{k-1})$. Since $c = (c_k)_{k \geq 0}$ satisfies (2.1), there exists a constant $\alpha_2 < \infty$ such that

$$\sup_{k \geq 1} \{ \|a_k\|_\infty \omega_k^{s+1} \} \leq \sup_{k \geq 1} \{ \frac{1}{2k} (\|c_{k+1}\|_\infty + \|c_{k-1}\|_\infty) \omega_k^{s+1} \} \leq \alpha_2.$$

That shows that $x = (x_k)_{k \geq k_0} \in X^{s+1}$. Repeating the same argument inductively and using the fact that $X^{s_1} \subset X^{s_2}$ for any $s_1 \geq s_2$, one gets that $x \in X^{s_0}$ for all $s_0 > 1$. Finally, the fact that $u(t) = a_0 + 2 \sum_{k \geq 1} a_k T_k(t)$ is a solution of $F = 0$ where F is the integral operator (1.7) (respectively (1.12)) if and only if $x = (x_k)_{k \geq k_0} \in X^s$ solves $f(x) = 0$ where f is the IVP-operator (1.9) (respectively the BVP-operator (1.13)) is trivial by construction. □

A consequence of Lemma 2.1 is that if one shows the existence of $x \in X^s$ such that $f(x) = 0$ (for some $s > 1$) where f is the IVP-operator (1.9) (respectively the BVP-operator (1.13)), then the coefficients $(a_k)_j$ decay faster than any algebraic decay and $u(t)$ given by (1.2) is a solution of the IVP defined by (1.1) and $u(-1) = p_0$ (respectively the BVP defined by (1.1) and (1.11)).

The strategy to find solutions of (1.6) is to consider an equivalent fixed point operator $T : X^s \to X^s$ whose fixed points are in one-to-one correspondence with the zeros of f. More precisely, the operator T is a Newton-like operator about an approximate solution $\bar{x}$ of f. In order to compute this numerical approximation we introduce a Galerkin projection. Let $m > 1$ and define the finite dimensional projection $\Pi_m : X^s \to X_m^s$ by $\Pi_m x = (x_k)_{k=k_0}^{m-1}$. The Galerkin projection of f is defined by

$$f^{(m)} : X_m^s \to X_m^s : x_F \mapsto \Pi_m f(x_F, 0_\infty), \tag{2.2}$$

where $0_\infty = (I - \Pi_m)0$. Identifying $(x_F, 0_\infty)$ with $x_F \in X_m^s \cong \mathbb{R}^{p+nm}$ we think of $f^{(m)} : \mathbb{R}^{p+nm} \to \mathbb{R}^{p+nm}$, where $p = 0$ for $k_0 = 0$. Now assume that we have computed $\bar{x}_F \in \mathbb{R}^{p+nm}$ such that $f^{(m)}(\bar{x}_F) \approx 0$ and let $\bar{x} = (\bar{x}_F, 0_\infty) \in X^s$. Let $B_{\bar{x}}(r) = \bar{x} + B(r)$, the closed ball in X^s of radius r centered at $\bar{x}$, where

$$B(r) = \left\{ x \in X^s : \ \|x\|_s = \sup_{k \geq k_0} \{ \|x_k\|_\infty \omega_k^s \} \leq r \right\} = \prod_{k \geq k_0} \left[-\frac{r}{\omega_k^s}, \frac{r}{\omega_k^s} \right]^{d(k)}, \tag{2.3}$$

where $d(-1) = p$ and $d(k) = n$ for $k \geq 0$. In order to define the fixed point operator T, we introduce $A_m \approx \left(Df^{(m)}(\bar{x}_F) \right)^{-1}$ a numerical inverse of $Df^{(m)}(\bar{x}_F)$. Assume that the finite dimensional matrix A_m is invertible (this hypothesis can be rigorously verified with interval arithmetic). Define the linear invertible operator $A : X^s \to X^{s+1}$ by

$$(Ax)_k = \begin{cases} (A_m(\Pi_m x))_k, & k = k_0, \ldots, m-1 \\ \left(\frac{1}{2k} \right) x_k, & k \geq m. \end{cases} \tag{2.4}$$

Define the Newton-like operator $T : X^s \to X^s$ about the numerical solution $\bar{x}$ by

$$T(x) = x - Af(x). \tag{2.5}$$

The goal is to determine (if possible) a positive radius r of the ball $B_{\bar{x}}(r)$ so that $T : B_{\bar{x}}(r) \to B_{\bar{x}}(r)$ is a contraction. Assuming that such an $r > 0$ exists, an application of the contraction mapping theorem yields the existence of a unique fixed point $\tilde{x}$ of T within the closed ball $B_{\bar{x}}(r)$. By invertibility of the linear operator A, one can conclude that $\tilde{x}$ is the unique solution of $f(x) = 0$ in the ball $B_{\bar{x}}(r)$. By construction, this unique solution represents a solution $u(t)$ of the IVP-operator (1.7) or the boundary value problem (1.12), depending on the situation. Hence, all we need to do is to find $r > 0$ such that $T : B_{\bar{x}}(r) \to B_{\bar{x}}(r)$ is a contraction. This task is achieved with the notion of the radii polynomials (originally introduced in [1] to compute equilibria of PDEs), which provide an efficient way of constructing a set on which the contraction mapping theorem is applicable. Their construction depends on some bounds that we introduce shortly. Before that, we introduce the notation $\preceq$ and $\prec$ to denote component-wise (strict) inequality, that is given two vectors $u, v \in \mathbb{R}^d$, $(d \geq 1)$, $u \preceq v$ if and only if $u_k \leq v_k$ for all $k = 1, \ldots, d$ and $u \prec v$ if and only if $u_k < v_k$ for all $k = 1, \ldots, d$. In addition we write for the component-wise absolute value of $y \in \mathbb{R}^d$ $|y| = (|y_1|, \ldots, |y_d|) \in \mathbb{R}^d$. Consider now the bound $Y = (Y_k)_{k \geq k_0}$ satisfying

$$\left| \left[T(\bar{x}) - \bar{x} \right]_k \right| \preceq Y_k, \quad k \geq k_0, \tag{2.6}$$

where $Y_k \in \mathbb{R}^n_+$ for $k \geq 0$. If $k_0 = -1$, then $Y_{k_0} \in \mathbb{R}^p_+$. Consider the bound $Z(r) = (Z_k(r))_{k \geq k_0}$ satisfying

$$\sup_{\xi_1, \xi_2 \in B(r)} \left| \left[DT(\bar{x} + \xi_1)\xi_2 \right]_k \right| \preceq Z_k(r), \quad k \geq k_0, \tag{2.7}$$

where $Z_k(r) \in \mathbb{R}^n_+$ for $k \geq 0$. If $k_0 = -1$, then $Z_{k_0}(r) \in \mathbb{R}^p_+$. If the vector field (1.1) is polynomial, then it is possible to obtain a polynomial expansion in r for $Z_k(r)$. As a matter of fact, in this case, the degree of the polynomial $Z_k(r)$ is the same as the degree of the polynomial vector field $\Psi(u)$. In case the analytic vector field $\Psi(u)$ is not polynomial, a rigorous general strategy to get a polynomial expression in r for $Z_k(r)$ would have to be incorporated in our approach. We now make the following important assumption. Assume that there exists a number $M \geq m$ where m is the *dimension* of the Galerkin projection (2.2) such that the bounds Y and Z satisfying (2.6) and (2.7) are such that

A1. $Y_k = 0 \in \mathbb{R}^n$ for all $k \geq M$.

A2. There exists a *uniform* polynomial bound $\bar{Z}_M(r) \in \mathbb{R}^n_+$ such that for all $k \geq M$,

$$Z_k(r) \preceq \frac{\bar{Z}_M(r)}{\omega_k^s}. \tag{2.8}$$

Before introducing the radii polynomials, let us briefly talk about these two assumptions. If the vector field $\Psi(u)$ is polynomial, then the nonlinear terms $c_k(\bar{a})$ are convolutions terms of the form $(\bar{a}_{(j_1)}\bar{a}_{(j_2)} \cdots \bar{a}_{(j_\ell)})_k$ which are eventually equal to zero for large enough k since $\bar{a}_k = 0$ for $k \geq m$. Hence, by construction of A defined in (2.4) and of the bound Y as in (2.6), there exists an M such that Y_k can be defined to be $0 \in \mathbb{R}^n$ for $k \geq M$. Again in case the vector field $\Psi(u)$ is polynomial, there are some analytic convolution estimates (e.g. the ones developed in [4]) that allow computing $\bar{Z}_M(r)$ satisfying (2.8). The computation of the uniform polynomial bound $\bar{Z}_M(r)$ is presented explicitly in the examples of Section 3.

DEFINITION 2.2. *Denote by* $\mathbf{1_n} \in \mathbb{R}^n$ *the vector whose components are all* 1. *We define the finite radii polynomials* $(p_k(r))_{k\geq k_0}^{M-1}$ *by*

$$p_k(r) = Y_k + Z_k(r) - \frac{r}{\omega_k^s}\mathbf{1_n}, \quad k = k_0, \ldots, M-1, \tag{2.9}$$

and the tail radii polynomial by

$$p_M(r) = \bar{Z}_M(r) - r\mathbf{1_n}. \tag{2.10}$$

The following result justifies the construction of the radii polynomials of Definition 2.2.

THEOREM 2.3. *If there exists* $r > 0$ *such that* $p_k(r) \prec 0$ *for all* $k = k_0, \ldots, M$, *then* $T : B_{\bar{x}}(r) \to B_{\bar{x}}(r)$ *is a contraction and therefore there exists a unique* $\tilde{x} \in B_{\bar{x}}(r)$ *such that* $T(\tilde{x}) = \tilde{x}$. *Hence, there exists a unique* $\tilde{x} \in B_{\bar{x}}(r)$ *such that* $f(\tilde{x}) = 0$.

Proof. See Corollary 3.6 in [4, 16, 1]. □

The strategy to rigorously compute solutions of the IVP-operator f given in (1.7) and the BVP-operator f given in (1.12) is therefore to construct the radii polynomials of Definition 2.2, to verify (if possible) the hypothesis of Theorem 2.3, and to use the result of Lemma 2.1 to conclude that $u(t) = a_0 + 2\sum_{k\geq 1} a_k T_k(t)$ is a solution of $F = 0$ where F is either the integral operator given by (1.7) or the operator given by (1.12)

While the computation of the bound Y satisfying (2.6) is rather straightforward, the computation of the polynomial bound $Z(r)$ satisfying (2.7) is more involved. In order to simplify its computation, we introduce the linear invertible operator $A^\dagger : X^s \to X^{s-1}$ by

$$(A^\dagger x)_k = \begin{cases} (Df^{(m)}(\bar{x}_F)(\Pi_m x))_k, & k = k_0, \ldots, m-1 \\ (2k)\, x_k, & k \geq m. \end{cases} \tag{2.11}$$

and we use the factorization $T(x) = x - Af(x) = (I - AA^\dagger)x - A(f(x) - A^\dagger x)$. Letting $\xi_1 = wr$, $\xi_2 = vr$ with $w, v \in B(1)$, one has that

$$\begin{aligned} DT(\bar{x} + \xi_1)\xi_2 &= (I - AA^\dagger)\xi_2 - A\left(Df(\bar{x} + \xi_1)\xi_2 - A^\dagger\xi_2\right) \\ &= \left[(I - AA^\dagger)v\right] r - A\left(Df(\bar{x} + wr)vr - A^\dagger vr\right), \end{aligned} \tag{2.12}$$

where the first term is of the form ϵr, for $\epsilon = (I - AA^\dagger)v \in X^s$ very small, and where the coefficient of r in $[Df(\bar{x} + wr)vr - A^\dagger vr]_k$ should be small as the dimension of the Galerkin projection m is large. Hence, for m large enough, the coefficient in r of $Z_k(r)$ should be small. That should increase the chances of the coefficient of r in the radii polynomials defined in Definition 2.2 to be negative, and therefore increase the chances of verifying the hypothesis of Theorem 2.3. We are now ready to present some applications.

3. Applications. In this section, we present two applications. The first application, presented in Section 3.1, concerns initial value problems in the Lorenz equations. More precisely, we use the notion of radii polynomials to compute rigorously solutions of the IVP-operator f given by (1.9). This yields rigorous enclosures of solutions of the integral operator (1.7), where $\Psi(u)$ is the vector field arising in the Lorenz equations. The second application, presented in Section 3.2, concerns projected boundary value problems in the Gray-Scott equation. More precisely, we use the notion of radii polynomials to compute rigorously solutions of the BVP-operator f given by (1.13) where one of the boundary value is in the stable manifold of a steady state. This yields rigorous enclosures of several symmetric connecting orbits for the Gray-Scott equation.

3.1. Initial value problem in the Lorenz equations. Consider the Lorenz equations re-scaled by a time factor L given by

$$\frac{du}{dt} = \Psi(u) = L \begin{pmatrix} \sigma(u_2 - u_1) \\ \rho u_1 - u_2 - u_1 u_3 \\ u_1 u_2 - \beta u_3 \end{pmatrix} \tag{3.1}$$

at the classical parameter values $\sigma = 10$, $\rho = 28$ and $\beta = 8/3$.

The Chebyshev coefficients (1.8) of (3.1) are given explicitly by

$$c_k = L \begin{pmatrix} \sigma((a_2)_k - (a_1)_k) \\ \rho(a_1)_k - (a_2)_k - (a_1 a_3)_k \\ (a_1 a_2)_k - \beta(a_3)_k \end{pmatrix} \tag{3.2}$$

with

$$(a_n a_m)_k = \sum_{\substack{k_1+k_2=k \\ k_i \in \mathbb{Z}}} (a_n)_{|k_1|}(a_m)_{|k_2|}$$

for $n = 1$, $m = 1, 2$ and $k \geq 0$. Given an initial condition p_0, this results in an explicit expression $f(x)$ for the IVP-operator (1.9). We now present rigorous numerical results illustrating the performance of our method.

THEOREM 3.1. *Consider*

$$\begin{aligned} p_0^1 &= (8.102574164767477, 9.551574461919124, 24.429705657930224) \\ p_0^2 &= (-0.208252089096454, -0.454566900892446, 0) \\ p_0^3 &= (4.102702069909453, 8.936495309135337, 0.5789130478426856). \end{aligned}$$

Let $s_1 = 2.5$, $s_2 = 2.7$ and $s_3 = 2.4$. For $p_0 \in \{p_0^1, p_0^2, p_0^3\}$ consider the IVP-operator f given by (1.9) *with c_k as in* (3.2)*. For each L in Table 3.1 there exists a unique solution $\tilde{x} \in X^{s_{1,2,3}}$ of $f(x) = 0$ in a ball $B_{\bar{x}}(\bar{r}_{p_0^{1,2,3}}) \subset X^s$ of radius $\bar{r}_{p_0^{1,2,3}}$ centered at an approximate solution $\bar{x}$.*

L	0.5	1	1.5	2	2.5	3
$m_{p_0^1}$	50	150	200	250	450	500
$m_{p_0^2}$	300	failed	failed	failed	failed	failed
$m_{p_0^3}$	100	200	400	500	failed	failed
$\bar{r}_{p_0^1}$	1.87×10^{-8}	2.19×10^{-7}	4.97×10^{-7}	1.15×10^{-6}	7.88×10^{-6}	1.01×10^{-5}
$\bar{r}_{p_0^2}$	9.87×10^{-6}	$--$	$--$	$--$	$--$	$--$
$\bar{r}_{p_0^3}$	6.79×10^{-7}	1.26×10^{-6}	8.57×10^{-6}	1.37×10^{-5}	$--$	$--$

Table 3.1: Given $p_0^{1,2,3}$ and a fixed L, these are corresponding values of the Galerkin projection dimension $m_{p_0^{1,2,3}}$ and the radius $\bar{r}_{p_0^{1,2,3}}$ of a ball around the approximate solution $\bar{x}$ in X^s in which the radii polynomials approach was successful. The number of modes $m_{p_0^{1,2,3}}$ one needs in order to find this ball where the mapping T is a contraction can be seen as a measure of numerical difficulty to run the proof. Note that the corresponding integration time is equal to $2L$, i.e. the corresponding solution u of the unrescaled equation (3.1) is defined on $[-L, L]$ with $u(-L) = p_0^{1,2,3}$.

Before we discuss the proof via an application of Theorem 2.3 we comment on the choice of the initial conditions: p_0^1 is chosen to lie approximately on the unstable

manifold of the *positive eye* equilibrium $(\sqrt{\beta(\rho-1)}, \sqrt{\beta(\rho-1)}, \rho-1)$, p_0^2 lies approximately on the unstable manifold of the origin whereas p_0^3 is taken randomly. As one can see in Table 3.1, the data of the verification method depends strongly on the choice of the initial condition. We assume that this stems from the presence of poles of the complex extension of the solutions $u : [-1,1] \to \mathbb{R}^3$ of (3.1) whose position in the complex plane changes depending on the initial condition and the scaling factor L. By Theorem 1.2 this influences the decay rate of the Chebyshev coefficients. This is illustrated in Figure 3.1. We refer to Figure 3.2 for a representation in phase space of two solutions of Theorem 3.1.

The proof of Theorem 3.1 can be found in the MATLAB programs *proofLorenz1.m*, *proofLorenz2.m* and *proofLorenz3.m* at [17]. It relies on Theorem 2.3 and uses the package Intlab [18] for the interval computations and the package Chebfun [19]. In order to apply Theorem 2.3 the construction of the radii polynomials as defined in (2.9) and (2.10) is crucial. After the following remark we aim to give some details about the derivation of the bounds defined in (2.6), (2.7) and (2.8) involved in the construction of the polynomials.

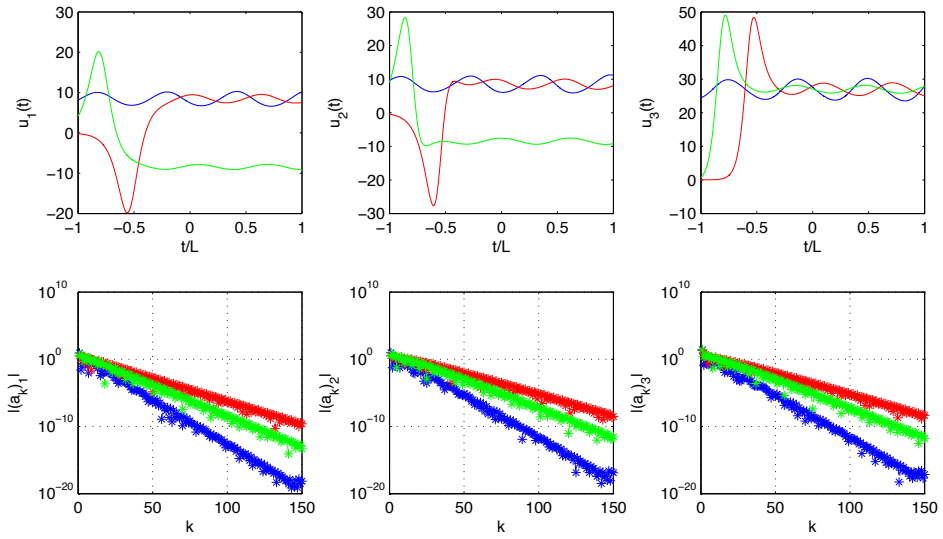

Fig. 3.1: Comparison of the componentwise solution profiles of a solution $u : [-1,1] \to \mathbb{R}^3$ of the Lorenz equations for the initial condition p_0^1 (blue), p_0^2 (red) and p_0^3 (green) for $L = 0.5$ and of the decay rates of their Chebyshev coefficient sequences.

REMARK 3.1. *Consider an approximate solution $\bar{x}$ and a corresponding unique genuine solution $\tilde{x} \in B_{\bar{x}}(r) \subset X^s$ of $f(x) = 0$ for a decay rate $s > 1$ and a radius $r > 0$. Via the expansion (1.2) the sequences of Chebyshev coefficients $\bar{x}$ and $\tilde{x}$ correspond to functions $\bar{u}$ and $\tilde{u}$ respectively, where $\tilde{u}$ solves (3.1) with respective initial condition p_0. Given $s > 1$, the inequality $\|\bar{x} - \tilde{x}\|_s \leq r$ can be used to get that*

$$\|\bar{u} - \tilde{u}\|_{C^0} \overset{\text{def}}{=} \sup_{t\in[-1,1]} \|\bar{u}(t) - \tilde{u}(t)\|_\infty \leq \|\bar{a}_0 - \tilde{a}_0\|_\infty + 2 \sup_{t\in[-1,1]} \sum_{k=1}^{\infty} \|\bar{a}_k - \tilde{a}_k\|_\infty \underbrace{|T_k(t)|}_{\leq 1}$$

$$\leq \left(1 + 2\sum_{k=1}^{\infty} \frac{1}{\omega_k^s}\right) r \leq \left(3 + \frac{2}{s-1}\right) r.$$

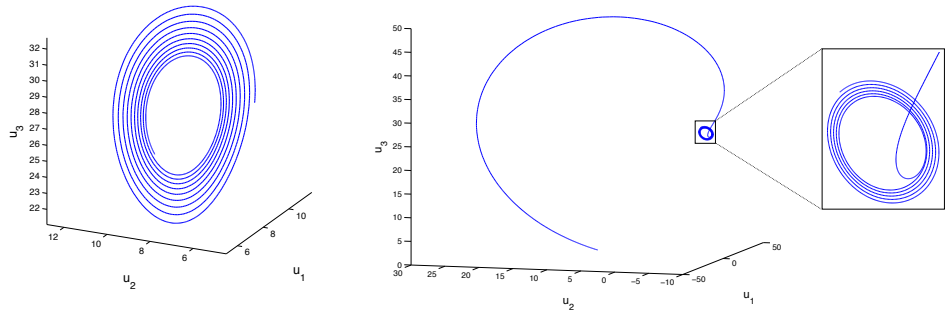

Fig. 3.2: Profile in phase space of the solution (u_1, u_2, u_3) of the Lorenz equations starting at (a) the initial condition p_0^1 for integration time 6 (corresponding to $L = 3$); (b) the initial condition p_0^3 for integration time 4 (corresponding to $L = 2$).

We now turn to the computations of the bounds involved in the construction of the radii polynomials.

3.1.1. Bounds required to construct the radii polynomials. Note here that $k_0 = 0$, $p = 0$ and $n = 3$. Choose a time scaling factor L. Consider f the IVP-operator (1.9) with c_k given in (3.2). Recalling (2.2), consider a Galerkin projection dimension m and an approximate solution $\bar{x} = \bar{a} = (\bar{a}_F, 0_\infty)$, that is $f^{(m)}(\bar{a}_F) \approx 0$. Set the computational parameter M arising in hypotheses **A1** and **A2** to $M = 2m - 1$. With this choice, **A1** is fulfilled and we can directly compute $Y_0, \ldots, Y_{M-1}$ from (2.6) using interval arithmetic. Concerning the computation of $Z_1(r), \ldots, Z_{M-1}(r)$ satisfying (2.7) and $\bar{Z}_M(r)$ satisfying (2.8) we follow a three step process.
The first step is to use (2.12) and to compute polynomials $z_k(r) = z_k^{(1)} r + z_k^{(2)} r^2$ for $k \geq 0$ with $z_k^{(l)} \in \mathbb{R}^3$, such that $\left[Df(\bar{x} + rw)rv - A^\dagger rv\right]_k = z_k(r)$, where $w, v \in B(1)$. Note that $B(1)$ is given by (2.3) with $r = 1$. We remark that we have to distinguish the cases $k = 0$, $1 \leq k \leq m-1$ and $m \leq k$. A straightforward calculation leads to the expressions summarized in Table 3.2. Note that v_i^I is defined for $i = 1, 2, 3$ by

$$(v_i^I)_k = \begin{cases} 0, & k = 0, \ldots, m-1 \\ (v_i)_k, & k \geq m. \end{cases}$$

Our next goal is to compute polynomials $\tilde{Z}_k(r) = \tilde{Z}_k^{(1)} r + \tilde{Z}_k^{(2)} r^2 \in \mathbb{R}^3$ such that

$$\left| z_k^{(l)} \right| \preceq \tilde{Z}_k^{(l)}, \quad \text{for } \; l = 1, 2 \; \text{ and } \; k = 0, \ldots, M-1 \tag{3.3}$$

and $\tilde{Z}_M(r) = \tilde{Z}_M^{(1)} r + \tilde{Z}_M^{(2)} r^2 \in \mathbb{R}^3$ such that

$$|z_k^{(l)}| \preceq \frac{\tilde{Z}_M^{(l)}}{\omega_k^s}, \quad \text{for } \; l = 1, 2 \; \text{ and } \; k \geq M. \tag{3.4}$$

To obtain the bounds $\tilde{Z}_k^{(1)}$ for $k = 0, \ldots, M-1$ define the finite sums

	$k=0$
$z_0^{(1)}$	$-2\sum_{j=m}^{\infty}(-1)^j v_j$
	$k=1,\dots,m-1$
$z_k^{(1)}$	$L\left[\begin{pmatrix}0\\ -(\bar a_3 v_1^I)_{k+1}-(\bar a_1 v_3^I)_{k+1}\\ (\bar a_1 v_2^I)_{k+1}+(\bar a_2 v_2^I)_{k+1}\end{pmatrix}-\begin{pmatrix}0\\ -(\bar a_3 v_1^I)_{k-1}-(\bar a_1 v_3^I)_{k-1}\\ (\bar a_1 v_2^I)_{k-1}+(\bar a_2 v_2^I)_{k-1}\end{pmatrix}\right]$
$z_k^{(2)}$	$L\left[\begin{pmatrix}0\\ -(w_3 v_1)_{k+1}-(w_1 v_3)_{k+1}\\ (w_1 v_2)_{k+1}+(w_2 v_1)_{k+1}\end{pmatrix}-\begin{pmatrix}0\\ -(w_3 v_1)_{k-1}-(w_1 v_3)_{k-1}\\ (w_1 v_2)_{k-1}+(w_2 v_1)_{k-1}\end{pmatrix}\right]$
	$k\geq m$
$z_k^{(1)}$	$L\left[\left[\begin{pmatrix}\sigma((v_2)_{k+1}-(v_1)_{k+1})\\ \rho(v_1)_{k+1}-(v_2)_{k+1}\\ -\beta(v_3)_{k+1}\end{pmatrix}+\begin{pmatrix}0\\ -(\bar a_3 v_1)_{k+1}-(\bar a_1 v_3)_{k+1}\\ (\bar a_1 v_2)_{k+1}+(\bar a_2 v_2)_{k+1}\end{pmatrix}\right]-\left[\begin{pmatrix}\sigma((v_2)_{k-1}-(v_1)_{k-1})\\ \rho(v_1)_{k-1}-(v_2)_{k-1}\\ -\beta(v_3)_{k-1}\end{pmatrix}+\begin{pmatrix}0\\ -(\bar a_3 v_1)_{k-1}-(\bar a_1 v_3)_{k-1}\\ (\bar a_1 v_2)_{k-1}+(\bar a_2 v_2)_{k-1}\end{pmatrix}\right]\right]$
$z_k^{(2)}$	$L\left[\begin{pmatrix}0\\ -(w_3 v_1)_{k+1}-(w_1 v_3)_{k+1}\\ (w_1 v_2)_{k+1}+(w_2 v_1)_{k+1}\end{pmatrix}-\begin{pmatrix}0\\ -(w_3 v_1)_{k-1}-(w_1 v_3)_{k-1}\\ (w_1 v_2)_{k-1}+(w_2 v_1)_{k-1}\end{pmatrix}\right]$

Table 3.2: Formulas for $z_k^{(l)}$, for $k\geq 0$ and for $l=1,2$.

$$\Sigma_i^{k,I}\stackrel{\text{def}}{=}\sum_{k_1=-m+1}^{m-1}(|\bar a_i|)_{|k_1|}\frac{1}{\omega^{s,I}_{|k-k_1|}},\quad \text{for}\quad k=0,\dots,M-1,$$
$$\Sigma_i^{k}\stackrel{\text{def}}{=}\sum_{k_1=-m+1}^{m-1}(|\bar a_i|)_{|k_1|}\frac{1}{\omega^{s}_{|k-k_1|}},\quad \text{for}\quad k=0,\dots,M,$$

where

$$\frac{1}{\omega_k^{s,I}}\stackrel{\text{def}}{=}\begin{cases}0, & 0\leq k\leq m-1\\ \frac{1}{\omega_k^s}, & k\geq m.\end{cases}$$

To define the uniform bound $\tilde Z_M^{(1)}$ for $k\geq M$ we set for $i=1,2,3$

$$\Sigma_i^{M-1}=(|\bar a_i|)_0+\sum_{k_1=1}^{m-1}(|\bar a_i|)_{k_1}\left(1+\frac{1}{(1-\frac{k_1}{M-1})^s}\right).$$

In order to compute $\tilde Z_k^{(2)}$ for $k=0,\dots,M$ and $\tilde Z_M^{(2)}$ we employ estimates whose detailed explanation can be found in [4]. For $M\geq 6$ and $s\geq 2$, define the constant

$$\gamma_M=2\left(\frac{M}{M-1}\right)^s+\left(\frac{4\ln(M-2)}{M}+\frac{\pi^2-6}{3}\right)\left(\frac{1}{M}+\frac{1}{2}\right)^{s-2},$$

and in addition define

$$\alpha_k^{2,M}=\begin{cases}1+2\sum_{k_1=1}^{M}\frac{1}{\omega_{k_1}^{2s}}+\frac{2}{M^{2s-1}(2s-1)}, & k=0\\ \sum_{k_1=1}^{M}\frac{2k^s}{\omega_{k_1}^s\omega_{k+k_1}^s}+\frac{2k^s}{(k+M+1)^s(M-1)^s(s-1)}+2+\sum_{k_1=1}^{M}\frac{2k^s}{\omega_{k_1}^s\omega_{k-k_1}^s}, & 1\leq k\leq M-1\\ 2+2\sum_{k_1=1}^{M}\frac{1}{\omega_{k_1}^s}+\frac{2}{M^{s-1}(s-1)}+\gamma_M, & k\geq M.\end{cases}$$

This yields that

$$\left| \sum_{k_1+k_2=k} \frac{1}{\omega_{k_1}\omega_{k_2}} \right| \leq \frac{\alpha_k^{2,M}}{\omega_k^s}, \quad \text{for} \quad k \geq 0.$$

One can use these definitions to obtain upper bounds for $|z_k(r)|$ $(k \geq 0)$. These new resulting bounds can be found in Table 3.3.

	$k = 0$
$\tilde{Z}_0^{(1)}$	$\frac{2}{(s-1)(m-1)^{s-1}} \begin{pmatrix} 1 \\ 1 \\ 1 \end{pmatrix}$
	$k = 1, \ldots, m-1$
$\tilde{Z}_k^{(1)}$	$\scriptstyle L \left[\begin{pmatrix} \Sigma_3^{k+1,I} & {}^{0} & + \Sigma_1^{k+1,I} \\ \Sigma_1^{k+1,I} & & + \Sigma_2^{k+1,I} \end{pmatrix} + \begin{pmatrix} \Sigma_3^{k-1,I} & {}^{0} & + \Sigma_1^{k-1,I} \\ \Sigma_1^{k-1,I} & & + \Sigma_2^{k-1,I} \end{pmatrix} \right]$
$\tilde{Z}_k^{(2)}$	$\scriptstyle L \left[\frac{\alpha_{k+1}^{2,M-1}}{\omega_{k+1}^s} + \frac{\alpha_{k-1}^{2,M-1}}{\omega_{k-1}^s} \right] \begin{pmatrix} 0 \\ 2 \\ 2 \end{pmatrix}$
	$k = m, \ldots, M-1$
$\tilde{Z}_k^{(1)}$	$\scriptstyle L \left[\frac{1}{\omega_{k+1}^s} \begin{pmatrix} 2\lvert\sigma\rvert \\ \lvert\rho\rvert + 1 \\ \lvert\beta\rvert \end{pmatrix} + \begin{pmatrix} \Sigma_3^{k+1} & {}^{0} & + \Sigma_1^{k+1} \\ \Sigma_1^{k+1} & & + \Sigma_2^{k+1} \end{pmatrix} \right] + L \left[\frac{1}{\omega_{k-1}^s} \begin{pmatrix} 2\lvert\sigma\rvert \\ \lvert\rho\rvert + 1 \\ \lvert\beta\rvert \end{pmatrix} + \begin{pmatrix} \Sigma_3^{k-1} & {}^{0} & + \Sigma_1^{k-1} \\ \Sigma_1^{k-1} & & + \Sigma_2^{k-1} \end{pmatrix} \right]$
$\tilde{Z}_k^{(2)}$	$\scriptstyle L \left[\frac{\alpha_{k+1}^{2,M-1}}{\omega_{k+1}^s} + \frac{\alpha_{k-1}^{2,M-1}}{\omega_{k-1}^s} \right] \begin{pmatrix} 0 \\ 2 \\ 2 \end{pmatrix}$
	$k = M$
$\tilde{Z}_M^{(1)}$	$\scriptstyle L \left[(1 + (\frac{M}{M-1})^s) \begin{pmatrix} 2\lvert\sigma\rvert \\ \lvert\rho\rvert + 1 \\ \lvert\beta\rvert \end{pmatrix} + (1 + (\frac{M}{M-1})^s) \begin{pmatrix} \Sigma_3^{M-1} & {}^{0} & + \Sigma_1^{M-1} \\ \Sigma_1^{M-1} & & + \Sigma_2^{M-1} \end{pmatrix} \right]$
$\tilde{Z}_M^{(2)}$	$\scriptstyle L \left[(1 + (\frac{M}{M-1})^s) \alpha_{M-1}^{2,M-1} \right] \begin{pmatrix} 0 \\ 2 \\ 2 \end{pmatrix}$

Table 3.3: Formulas for $\tilde{Z}_k^{(l)}$, for $k = 0, \ldots, M$ and for $l = 1, 2$.

We are now in position to take the last step in defining $Z_k(r) = Z_k^{(1)} r + Z_k^{(2)} r^2$ for $k = 0, \ldots, M-1$ specified in (2.7) and $\bar{Z}_M(r) = \bar{Z}_M^{(1)} r + \bar{Z}_M^{(2)} r^2$ given by (2.8). As previously mentioned, by definition of A and $A^\dagger$, there is a small ϵ such that for all $k \geq 0$,

$$\left| \left[(I - AA^\dagger) rv \right]_k \right| \preceq r\epsilon \mathbf{1_3}.$$

In particular for $k \geq m$ we have $\epsilon = 0$ by definition of A and $A^\dagger$ given respectively by (2.4) and (2.11). We let $V_l = (\tilde{Z}_0^{(l)}, \ldots, \tilde{Z}_{m-1}^{(l)}) \in \mathbb{R}^{3m}$ for $l = 1, 2$ to obtain for $k = 0, \ldots, m-1$

$$\begin{aligned} Z_k^{(1)} &= \left[|A_m| V_1 \right]_k + \epsilon \mathbf{1_3} \\ Z_k^{(2)} &= \left[|A_m| V_2 \right]_k, \end{aligned} \tag{3.5}$$

where the absolute value is taken component-wise and for $k = m, \ldots, M-1$

$$Z_k^{(l)} = \frac{1}{2k} \tilde{Z}_k^{(l)}, \quad \text{for} \quad l = 1, 2. \tag{3.6}$$

Finally we set

$$\bar{Z}_M^{(l)} = \frac{1}{2M} \tilde{Z}_M^{(l)}, \quad \text{for} \quad l = 1, 2. \tag{3.7}$$

Combining the bounds $Y_0, \ldots, Y_{M-1}$ and the bounds (3.5), (3.6) and (3.7) completes the construction of the radii polynomials defined in (2.9) and (2.10).

3.2. The Gray-Scott equation. Consider the Gray-Scott equation re-scaled by a time factor L given by

$$\begin{cases} v_1'' = L^2\left(v_1 v_2^2 - \lambda(1-v_1)\right) \\ v_2'' = L^2\left(\frac{1}{\gamma}(v_2 - v_1 v_2^2)\right), \end{cases} \tag{3.8}$$

where γ and λ are real parameters. The Gray-Scott system serves as a model for a continuously fed unstirred autocatalytic reaction. The homoclinic solutions we seek represent non-trivial stationary spatial patterns in the form of pulses. See [23] and the references therein for more details on the significance of the equation. Letting $u_1 = v_1$, $u_2 = v_1'$, $u_3 = v_2$, $u_4 = v_2'$ and $u = (u_1, u_2, u_3, u_4)^T$, we re-write (3.8) as the vector field

$$\frac{du}{dt} = \Psi(u) = \begin{pmatrix} u_2 \\ L^2\left(\lambda u_1 + u_1 u_3^2 - \lambda\right) \\ u_4 \\ L^2\left(\frac{1}{\gamma}u_3 - \frac{1}{\gamma}u_1 u_3^2\right) \end{pmatrix}. \tag{3.9}$$

Hence, the Chebyshev coefficients (1.8) of (3.9) are given explicitly by

$$c_k = \begin{pmatrix} (a_2)_k \\ L^2\left(\lambda(a_1)_k + (a_1 a_3^2)_k - \lambda\delta_{k,0}\right) \\ (a_4)_k \\ L^2\left(\frac{1}{\gamma}(a_3)_k - \frac{1}{\gamma}(a_1 a_3^2)_k\right) \end{pmatrix}, \tag{3.10}$$

where $\delta_{k,0}$ is the Kronecker delta function and where

$$(a_1 a_3^2)_k = \sum_{\substack{k_1+k_2+k_3=k \\ k_i \in \mathbb{Z}}} (a_1)_{|k_1|}(a_3)_{|k_2|}(a_3)_{|k_3|}.$$

We are interested in computing symmetric homoclinic orbits at $p = (1,0,0,0)^T$. Consider $P(\theta)$ to be a parameterization of the local stable manifold $W^s_{\text{loc}}(p)$ at the steady state p. In order to compute P we employ the parametrization method developed in [24], [25] and [26]. The philosophy is to use a power series expansion to solve an invariance equation for P and thereby compute a multivariate polynomial approximation P_N to P. In addition the a-posteriori verification enables to find a domain V and a bound δ such that $\|P(\theta) - P_N(\theta)\|_\infty < \delta$ for all $\theta \in V$. For details on the implementation and the a-posteriori verification we refer the reader to [27].

We interpret symmetric homoclinic orbits as solutions of a BVP with the boundary value $u(1) = P(\theta)$, that is $u(1) \in W^s_{\text{loc}}(p)$. We impose an even symmetry condition of the orbit (v_1, v_2) with $v_1'(-1) = u_2(-1) = 0$ and $v_2'(-1) = u_4(-1) = 0$. Hence, the boundary condition (1.11) reads as $\mathcal{G}(u(-1), u(1)) = (u_2(-1), u_4(-1))^T \in \mathbb{R}^2$, $p_1 = P(\theta)$ and then the operator (1.12) is given by

$$F(\theta, u)(t) = \begin{pmatrix} u_2(-1) \\ u_4(-1) \\ u(t) + \displaystyle\int_t^1 \Psi(u(s))ds - P(\theta) \end{pmatrix}. \tag{3.11}$$

To obtain the first component η of (1.13), we use that $T_k(-1) = (-1)^k$ for all $k \geq 0$ to get

$$\eta(\theta, a) = \left((a_2)_0 + 2\sum_{k=1}^{\infty}(-1)^k (a_2)_k, (a_4)_0 + 2\sum_{k=1}^{\infty}(-1)^k (a_4)_k \right)^T. \tag{3.12}$$

Together with (3.10) we obtain an explicit expression $f(x) = f_{\gamma,\lambda}(x)$ for the BVP-operator (1.13) tailored to the problem of finding even homoclinics in the Gray-Scott system (3.9).

It is shown in [23] that for parameter values $\gamma\lambda = 1$ and $\lambda > 4$ there exists a family of even symmetric homoclinics. More precisely for all (λ, γ) in the parameter set

$$\mathcal{C}_0 = \left\{ (\gamma, \frac{1}{\gamma}) : \ 0 < \gamma < \frac{2}{9} \right\},$$

the functions given by

$$v_1(t) = 1 - \frac{3\gamma}{1 + Q\cosh(\frac{t}{\sqrt{\gamma}})} \quad \text{and} \quad v_2(t) = \frac{3}{1 + Q\cosh(\frac{t}{\sqrt{\gamma}})}, \tag{3.13}$$

with $Q(\gamma) = \sqrt{1 - \frac{9\gamma}{2}}$, are even symmetric homoclinic orbits of (3.9). Furthermore in Theorem C of [23] it is ensured that the homoclinics persist if $\lambda\gamma = 1 + \epsilon$ for some small ϵ and in [27] to a certain extent the magnitude of ϵ for $\gamma = 0.15$ is investigated. More concretely the authors of [27] show in Theorem 1.1 the existence of 30 homoclinic orbits on the line $\gamma = 0.15$ in parameter space. We take a similar approach but extend the considered region in parameter space. Before presenting the result, note that there is a theoretical constraint in using the parameterization method to compute $W^s_{\text{loc}}(p)$ in parameter space. This constraint comes from the presence of resonances between the eigenvalues $\pm\frac{L}{\sqrt{\gamma}}$ and $\pm\sqrt{\lambda}L$ of $D\Psi(p)$. A resonance occurs when $\lambda\gamma = n^2$ or $\lambda\gamma = (1/n)^2$ for some $n \in \mathbb{N}$. Denote $\mathcal{C}_n \stackrel{\text{def}}{=} \{(\lambda, \gamma) : \lambda\gamma = (n+1)^2\}$ for $n \geq 0$ and $\mathcal{C}_{1/n} \stackrel{\text{def}}{=} \{(\lambda, \gamma) : \lambda\gamma = (1/n)^2\}$ for $n \geq 2$. The power series representation of $W^s_{\text{loc}}(p)$ that the parameterization method uses, will fail to converge at resonances. As a matter of fact our rigorous numerical method combining Chebyshev series and the parameterization method will necessarily fail at those parameter values located on $\mathcal{C}_n$ $(n \geq 1)$ and $\mathcal{C}_{1/n}$ $(n \geq 2)$. Let us now formulate a result guaranteeing the existence of 2159 homoclinics for $\gamma \in \{0.10, \ldots, 0.20\}$, and for several different values of λ.

THEOREM 3.2. *Define*

$$\Lambda^{\pm}_{\mathcal{I},\Delta_\lambda}(\gamma) = \left\{ (\gamma, \lambda) : \lambda = \frac{1 \pm k\Delta_\lambda}{\gamma}, \ \ k \in \mathcal{I} \right\},$$

over an index set $\mathcal{I}$. Let $\Delta_\lambda = 0.03$ and $\gamma_i = 0.10 + (i-1)0.01$ for $i = 1, \ldots, 11$. Set $\mathcal{I}^+(\gamma_i) = \{1, \ldots, K^+(\gamma_i)\}$ and $\mathcal{I}^-(\gamma_i) = \{1, \ldots, K^-(\gamma_i)\}$ for $i = 1, \ldots, 11$, where $K^{\pm}(\gamma_i)$ is specified in Table 3.4. If

$$(\lambda, \gamma) \in \bigcup_{i=1}^{11} \Lambda^+_{\mathcal{I}^+(\gamma_i),\Delta_\lambda}(\gamma_i) \cup \Lambda^-_{\mathcal{I}^-(\gamma_i),\Delta_\lambda}(\gamma_i),$$

there exists a ball $B_{\bar{x}}(r_{\gamma,\lambda}) \subset X^s$ *(with* $f_{\gamma,\lambda}(\bar{x}) \approx 0$*) containing a unique solution* $\tilde{x} = (\tilde{\theta}, \tilde{a})$ *of* $f_{\gamma,\lambda}(x) = 0$ *corresponding to an even homoclinic solution of* (3.8).

For a geometric representation of the result of Theorem 3.2, we refer to Figure 3.3 and Figure 3.4.

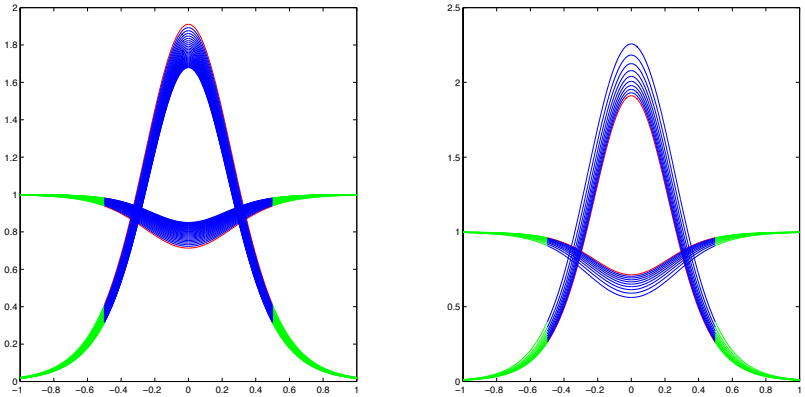

Fig. 3.3: Thirty-nine homoclinics from Theorem 3.2, where $(\lambda, \gamma) \in \Lambda^+_{\{1,\dots,30\},0.03}(0.15)$ on the left and $(\lambda, \gamma) \in \Lambda^-_{\{1,\dots,9\},0.03}(0.15)$ on the right. The red solution corresponds to the exact homoclinic given by (3.13). Each couple (v_1, v_2) is the center of a ball in function space in which an exact solution is guaranteed to exist. The blue part over $[0, \frac{1}{2}]$ corresponds to the interval $[-1, 1]$ for the operator (3.11), which in turn corresponds to the rescaling of $[0, L^{\pm}(0.15)]$. The green part is added by using the conjugacy relation (see equation (57) in [27]) fulfilled by the parametrization P of $W^s_{\mathrm{loc}}(p)$, where we integrate for 2 time units on the time scale of (3.11) and then rescale $[-1, 3]$ to the interval [0,1]. The part over $[-1, 0]$ is obtained using the symmetry.

γ	0.10	0.11	0.12	0.13	0.14	0.15	0.16	0.17	0.18	0.19	0.20
$L^+(\gamma)$	0.45	0.50	0.55	0.60	0.60	0.60	0.65	0.70	0.75	0.75	0.75
$L^-(\gamma)$	0.50	0.55	0.55	0.55	0.60	0.70	0.65	0.65	0.70	0.70	0.7
$K^+(\gamma)$	114	128	143	158	172	187	202	217	231	246	261
$K^-(\gamma)$	18	16	15	12	11	9	7	6	3	2	1

Table 3.4: Depending on the value of γ the rescaling factor L and the number of steps $K^{\pm}$ we take in the λ-directions is shown.

The rigorous verification of Theorem 3.2 can be found in the MATLAB programs *proofLambdaplus*γ*.m* and *proofLambdaminus*γ*.m* with $\gamma = 010, \dots, 020$ and relies on Theorem 2.3. All codes can be downloaded from [17]. The programs make use of the package Intlab [18] for the interval computations and of the package Chebfun [19]. Chebfun is used to compute the Chebyshev coefficients of the exact solutions (3.13) from which a continuation is performed. The main prerequisite for applying Theorem 2.3 is the construction of the radii polynomials (2.9) and (2.10). We now give some details on their derivation.

3.2.1. Bounds required to construct the radii polynomials. We are in the case $k_0 = -1$, $p = 2$ and $n = 4$. Consider a dimension m for the Galerkin projection

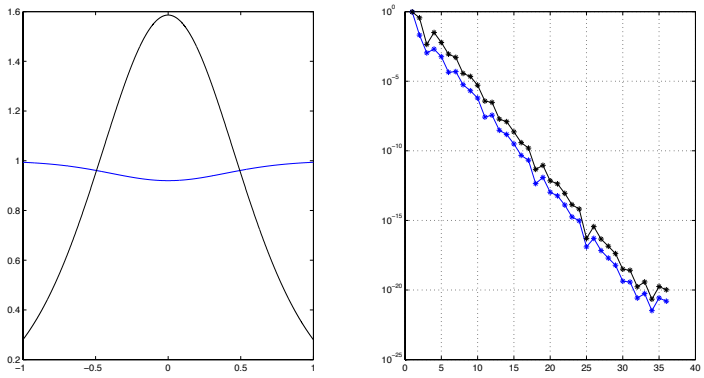

Fig. 3.4: **(Left)** Components v_1 (black) and v_2 (blue) of the homoclinic solution of Theorem 3.2 corresponding to the parameter value $(\gamma, \lambda) = (0.15, \frac{1+89(0.03)}{0.15}) \in \Lambda^+_{\mathcal{I}^+(0.15),0.03}(0.15)$. The interval $[0, 1]$ corresponds to the rescaled interval $[-1, 1]$ of (3.11), corresponding itself in turn to a rescaling of $[0, 0.6]$. The interval $[-1, 0]$ is added by symmetry. **(Right)** The Chebyshev coefficients of v_1 (black) and v_2 (blue). Notice the fast decay of the coefficients to zero.

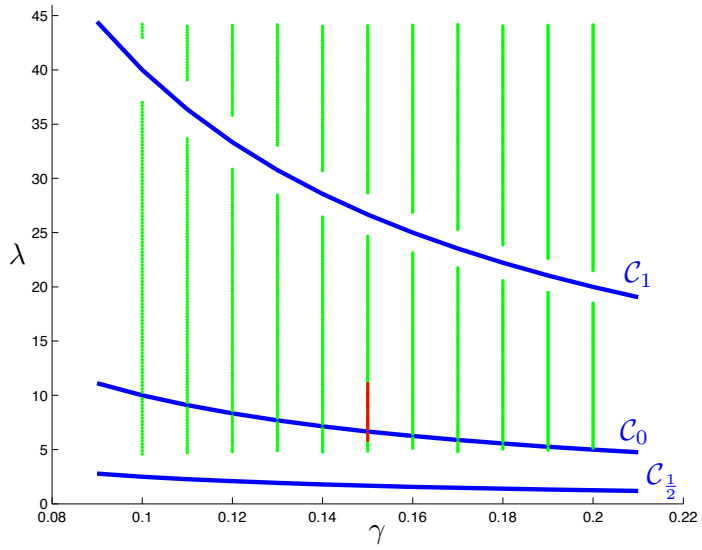

Fig. 3.5: The green points indicate the region in parameter space at which the rigorous proof of existence of symmetric homoclinics was obtained by computing the radii polynomials with interval arithmetic. The red points indicate the region investigated in [27]. Based on the discussion about resonances, we portrait the curve $\mathcal{C}_1$ and $C_{\frac{1}{2}}$ at which our rigorous method will necessarily fail. Note that $\mathcal{C}_0$ is the curve on which the exact homoclinics (3.13) exist.

(2.2) and an approximation $\bar{x} = (\bar{\theta}, \bar{a}) = (\bar{\theta}, \bar{a}_F, 0_\infty)$ such that $f^{(m)}(\bar{\theta}, \bar{a}_F) \approx 0$, where f is the BVP-operator (1.13), c_k is given in (3.10) and the boundary conditions $\eta : X^s \to \mathbb{R}^p$ is given by (3.12). For instance if $(\gamma, \lambda) \in \Lambda^+_{\mathcal{I}^+(0.15),\Delta_\lambda}$ we choose $m = 37$

and set $L = 0.6$. For $(\gamma, \lambda) \in \Lambda^-_{\mathcal{I}^-(0.15),\Delta_\lambda}$ we choose $m = 47$ and let $L = 0.7$. Note that if we set $M = 3m-2$ assumption **A1** is satisfied and $Y_1, \ldots, Y_M$ can be computed by (2.6). The strategy to construct the bounds $Z_1(r), \ldots, Z_{M-1}(r)$ and $\bar{Z}_M(r)$ defined in (2.7) and (2.8) is analogue to the Lorenz example. Note that ξ_1, ξ_2 in (2.12) are now given by $\xi_1 = r(\theta, w)$ and $\xi_2 = r(\phi, v)$ with $(\theta, w), (\phi, v) \in B(1) \subset X^s$. In addition we assume that we have a bound $\Lambda \in \mathbb{R}^4_+$ such that for every θ, ϕ corresponding to $\xi_{1,2}$

$$|DP(\bar{\theta} + r\theta)\phi| \preceq \Lambda$$

for all r with $0 < r < r_*$, where r_* is an apriori bound on r that we set to $r_* = 0.004$. The explicit construction of Λ in the context of the Gray-Scott equations is presented in Section 5 in [27]. In particular, at $(\gamma, \lambda) \in \Lambda^+_{\mathcal{I}^+(0.15),\Delta_\lambda}$ we choose $N = 13$ as the order of the polynomial approximation P_N and at $(\gamma, \lambda) \in \Lambda^-_{\mathcal{I}^-(0.15),\Delta_\lambda}$, we choose $N = 15$. For more details on the choice of m and N at $\gamma = 0.14, 0.16$ we refer to the code at [17]. A central step is to compute the polynomials $\tilde{Z}_k(r) = \sum_{l=1}^3 \tilde{Z}_k^{(l)} r^l \in \mathbb{R}^4$ and $\tilde{Z}_M(r) = \sum_{l=1}^3 \tilde{Z}_M^{(l)} r^l \in \mathbb{R}^4$ fulfilling the analogue of (3.3) and (3.4). We only present $\tilde{Z}_k^{(l)}$ and $\tilde{Z}_M^{(l)}$ for $k = 0, \ldots, M-1$ and $l = 1, 2, 3$ in Table A.1 in the Appendix.

Our main technical tool to compute these bounds is given by the following Lemma which is a simplified combination of Lemmas A.3 and A.4 in [4]. In order to explain its usefulness in our context, we recall that given three sequences $a, b, c \in \Omega^s$, the cubic convolution sums $(abc)_k$ can be split as

$$(abc)_k = (abc)_k^M + \sum_{\substack{k_1+k_2+k_3=k \\ \max\{|k_1|,|k_2|,|k_3|\} \geq M \\ k_i \in \mathbb{Z}}} a_{|k_1|} b_{|k_2|} c_{|k_3|},$$

where

$$(abc)_k^M \stackrel{\text{def}}{=} \sum_{\substack{k_1+k_2+k_3=k \\ |k_i| \leq M, i=1,2,3 \\ k_i \in \mathbb{Z}}} a_{|k_1|} b_{|k_2|} c_{|k_3|}.$$

One of the aims of the following result is to bound the infinite tail sum.

LEMMA 3.3. *Let $a, b, c \in \Omega^s$ and $M \geq 6$. Set $A = \|a\|_s$, $B = \|b\|_s$ and $C = \|c\|_s$. Then there exist computable numbers $\varepsilon_k^{(3)} = \varepsilon_k^{(3)}(M)$ for $k = 0, \ldots, M$ such that*

$$\sum_{\substack{k_1+k_2+k_3=k \\ \max\{|k_1|,|k_2|,|k_3|\} \geq M+1 \\ k_i \in \mathbb{Z}}} |a|_{|k_1|} |b|_{|k_2|} |c|_{|k_3|} \leq 3(ABC)\varepsilon_k^{(3)}.$$

In addition there is a computable number $\alpha_{M-1}^{(3)}$ such that for $k \geq M-1$

$$\sum_{\substack{k_1+k_2+k_3=k \\ k_i \in \mathbb{Z}}} |a|_{|k_1|} |b|_{|k_2|} |c|_{|k_3|} \leq (ABC) \frac{\alpha_{M-1}^{(3)}}{\omega_k^s}.$$

For a proof and for details on the computation see [4] as well as the code at [17]. Defining $A_{1,3} = \|\bar{a}_{1,3}\|_s$ and for $i = 1, 3$ and $j = 3$

$$\Sigma_{ij}^{M-1} = \sum_{k_1=-m+1}^{m-1} \sum_{k_2=-m+1}^{m-1} (|\bar{a}_i|)_{|k_1|} (|\bar{a}_j|)_{|k_2|} \max\left\{ \frac{M^s}{(M-1-k_1-k_2)^s}, 1 \right\}$$

completes the ingredients for Table A.1.

4. Conclusion. Let us conclude this paper by presenting some potential extensions and improvements of our proposed rigorous computational method to solve IVPs and BVPs of ODEs.

First, our method could probably be generalized to compute rigorously solutions of higher-order differential equations without re-writing them as first order vector fields. For example, we believe that computing solutions of BVPs associated to the Gray-Scott equations (3.8) could be obtained by integrating twice each equation which could then be solved rigorously by moving to the space of Chebyshev coefficients. The improvement would be twofold. First, the linear part of the equations would grow as $O(k^2)$ (as opposed to $O(k)$ in the BVP-operator (1.13)), hence facilitating the use of a contraction mapping argument based on a Newton-like operator. Second, the size of the finite dimensional projection would be twice smaller. A downside is that we would obtain more complicated formulas for the Chebyshev expansions of the equations resulting from the double integration.

A second extension of the method would be to use a multiple shooting approach to solve the integral operators over long periods of time. Indeed, the theory of the Chebyshev series presented in Section 1 suggests that integrating over long periods of time (e.g. compute solutions with large scaling factor L) has the disadvantage of bringing the (potentially existing) poles closer to the ρ-ellipse mentioned in Theorem 1.2. This implies that the Chebyshev coefficients of the solutions decay to zero at a slow rate. Therefore, an advantage of a multiple shooting approach based on integrating over many short intervals (with corresponding short scaling factor L) would push away the poles, hence bringing a faster decay rate to the Chebyshev coefficients of the solutions. We could then potentially take smaller Galerkin projection dimensions to perform our rigorous computations, thanks to the fast decay rates of the solutions on each sub-intervals. The downside would again be a more complicated formulation of the operators which would need to take care of solving simultaneously many parallel problems.

A third extension of the method would be to combine the rigorous pseudo arc length continuation method of [16, 28] with the methods described in the present work to compute global smooth branches of solutions of BVPs.

A fourth and slightly more challenging improvement consists of modifying the proposed approach to vector fields with nonlinearities that are non polynomial. That would require extending the already existing convolution estimates to the non polynomial case.

A final and most ambitious extension would be to attempt to rigorously compute solutions of spatially periodic PDEs combining a Chebyshev series expansion in time and a Fourier series expansion in space.

Acknowledgements. The authors would like to thank the anonymous referee for very helpful comments that strongly helped the presentation of the paper. Special thanks to Michel Lapointe from Laval University who helped with setting up the computations for the Gray-Scott equation.

REFERENCES

[1] Sarah Day, Jean-Philippe Lessard, and Konstantin Mischaikow. Validated continuation for equilibria of PDEs. *SIAM J. Numer. Anal.*, 45(4):1398–1424 (electronic), 2007.

[2] Anthony W. Baker, Michael Dellnitz, and Oliver Junge. A topological method for rigorously computing periodic orbits using Fourier modes. *Discrete Contin. Dyn. Syst.*, 13(4):901–920, 2005.

[3] Jan Bouwe van den Berg and Jean-Philippe Lessard. Chaotic braided solutions via rigorous numerics: chaos in the Swift-Hohenberg equation. *SIAM J. Appl. Dyn. Syst.*, 7(3):988–1031, 2008.

[4] Marcio Gameiro and Jean-Philippe Lessard. Analytic estimates and rigorous continuation for equilibria of higher-dimensional PDEs. *J. Differential Equations*, 249(9):2237–2268, 2010.

[5] Mitsuhiro T. Nakao, Kouji Hashimoto, and Kenta Kobayashi. Verified numerical computation of solutions for the stationary Navier-Stokes equation in nonconvex polygonal domains. *Hokkaido Math. J.*, 36(4):777–799, 2007.

[6] Piotr Zgliczyński and Konstantin Mischaikow. Rigorous numerics for partial differential equations: the Kuramoto-Sivashinsky equation. *Found. Comput. Math.*, 1(3):255–288, 2001.

[7] Stanislaus Maier-Paape, Ulrich Miller, Konstantin Mischaikow, and Thomas Wanner. Rigorous numerics for the Cahn-Hilliard equation on the unit square. *Rev. Mat. Complut.*, 21(2):351–426, 2008.

[8] Jean-Philippe Lessard. Recent advances about the uniqueness of the slowly oscillating periodic solutions of Wright's equation. *J. Differential Equations*, 248(5):992–1016, 2010.

[9] Mikołaj Zalewski. Computer-assisted proof of a periodic solution in a nonlinear feedback DDE. *Topol. Methods Nonlinear Anal.*, 33(2):373–393, 2009.

[10] S. Day, O. Junge, and K. Mischaikow. A rigorous numerical method for the global analysis of infinite-dimensional discrete dynamical systems. *SIAM J. Appl. Dyn. Syst.*, 3(2):117–160 (electronic), 2004.

[11] S. Day, B. Kallies, Rigorous computation of the global dynamics of integrodifference equations with smooth nonlinearities, S. Day and W. D. Kalies. Accepted and to appear in SIAM Journal on Numerical Analysis, 2013.

[12] John P. Boyd. *Chebyshev and Fourier spectral methods*. Dover Publications Inc., Mineola, NY, second edition, 2001.

[13] Sara Day, Yasuaki Hiraoka, Konstantin Mischaikow, and Toshi Ogawa. Rigorous numerics for global dynamics: a study of the Swift-Hohenberg equation. *SIAM J. Appl. Dyn. Syst.*, 4(1):1–31 (electronic), 2005.

[14] Nicolas Brisebarre and Mioara Joldeş. Chebyshev interpolation polynomial-based tools for rigorous computing. In *ISSAC 2010—Proceedings of the 2010 International Symposium on Symbolic and Algebraic Computation*, pages 147–154. ACM, New York, 2010.

[15] L. N. Trefethen. *Approximation theory and approximation practice*. Society for Industrial and Applied Mathematics (SIAM), 2012.

[16] Maxime Breden, Jean-Philippe Lessard, and Matthieu Vanicat. Global bifurcation diagrams of steady states of systems of PDEs via rigorous numerics: a 3-component reaction-diffusion system. *Acta Mathematicae Applicandae*, 2013. Accepted.

[17] Jean-Philippe Lessard, and Christian Reinhardt. MATLAB code for the computation of solutions of nonlinear ODEs using Chebyshev polynomials. `http://archimede.mat.ulaval.ca/jplessard/chebyshev`

[18] S.M. Rump. INTLAB - INTerval LABoratory. In Tibor Csendes, editor, *Developments in Reliable Computing*, pages 77–104. Kluwer Academic Publishers, Dordrecht, 1999. http://www.ti3.tu-harburg.de/rump/.

[19] L. N. Trefethen et al. *Chebfun Version 4.2*. The Chebfun Development Team, 2011. `http://www.maths.ox.ac.uk/chebfun/`.

[20] L. N. Trefethen. Spectral methods in MATLAB. SIAM, Philadelphia, 2000.

[21] J.A.C. Weidemann, S.C. Reddy. A MATLAB Differentiation Matrix Suite. ACM Transactions of Mathematical Software,Vol. 26, pp. 465–519 (2000).

[22] Gottlieb, D., Hussaini, M. Y., and Orszag, S. A. 1984. Theory and applications of spectral-methods. In Spectral Methods for Partial Differential Equations, R. Voigt, D. Gottlieb, and M. Hussaini, Eds. 1-54.

[23] J. K. Hale, L. A. Peletier, and W. C. Troy. Exact homoclinic and heteroclinic solutions of the Gray-Scott model for autocatalysis. *SIAM J. Appl. Math.*, 61(1):102–130 (electronic), 2000.

[24] X. Cabré, E. Fontich, and R. de la Llave. The parameterization method for invariant manifolds. I. Manifolds associated to non-resonant subspaces. *Indiana Univ. Math. J.*, 52(2):283–328, 2003.

[25] X. Cabré, E. Fontich, and R. de la Llave. The parameterization method for invariant manifolds. II. Regularity with respect to parameters. *Indiana Univ. Math. J.*, 52(2):329–360, 2003.

[26] X. Cabré, E. Fontich, and R. de la Llave. The parameterization method for invariant manifolds. III. Overview and applications. *J. Differential Equations*, 218(2):444–515, 2005.

[27] Jan Bouwe van den Berg, Jason D. Mireles-James, Jean-Philippe Lessard, and Konstantin Mischaikow. Rigorous numerics for symmetric connecting orbits: even homoclinics of the

Gray-Scott equation. *SIAM J. Math. Anal.*, 43(4):1557–1594, 2011.

[28] Jan Bouwe van den Berg, Jean-Philippe Lessard, and Konstantin Mischaikow. Global smooth solution curves using rigorous branch following. *Math. Comp.*, 79(271):1565–1584, 2010.

Appendix A. Formulas for $\tilde{Z}_k$ for $k = -1, \ldots, M$ in the Gray-Scott equations. We give an overview of the bounds $\tilde{Z}_k$ for $k = -1, \ldots, M$ involved in the construction of the radii polynomials for the proof of Theorem 3.2.

	$k=-1$
$\tilde{Z}_{-1}^{(1)}$	$\frac{2}{(s-1)(m-1)^{s-1}}\begin{pmatrix}1\\1\end{pmatrix}$
	$k=0$
$\tilde{Z}_{0}^{(1)}$	$\frac{2}{(s-1)m^{s-1}}\begin{pmatrix}1\\1\\1\end{pmatrix}+\Lambda$
	$k=1,\dots,m-1$
$\tilde{Z}_{k}^{(1)}$	$\left[\begin{pmatrix}0\\ L^2((\lvert\bar{a}_3\rvert^2\lvert v_1\rvert^I)_{k+1}^M+2(\lvert\bar{a}_1\rvert\lvert\bar{a}_3\rvert\lvert v_3^I\rvert)_{k+1}^M)\\0\\ \frac{L^2}{\gamma}\left[(\lvert\bar{a}_3\rvert^2\lvert v_1\rvert^I)_{k+1}^M+2(\lvert\bar{a}_1\rvert\lvert\bar{a}_3\rvert\lvert v_3^I\rvert)_{k+1}^M\right]\end{pmatrix}+\varepsilon_{k+1}^{(3)}\begin{pmatrix}0\\ L^2(A_3+2A_1A_3)\\0\\ \frac{L^2}{\gamma}(A_3+2A_1A_3)\end{pmatrix}\right.$ $\left.+\begin{pmatrix}0\\ L^2((\lvert\bar{a}_3\rvert^2\lvert v_1\rvert^I)_{k-1}^M+2(\lvert\bar{a}_1\rvert\lvert\bar{a}_3\rvert\lvert v_3^I\rvert)_{k-1}^M)\\0\\ \frac{L^2}{\gamma}\left[(\lvert\bar{a}_3\rvert^2\lvert v_1\rvert^I)_{k-1}^M+2(\lvert\bar{a}_1\rvert\lvert\bar{a}_3\rvert\lvert v_3^I\rvert)_{k-1}^M\right]\end{pmatrix}+\varepsilon_{k-1}^{(3)}\begin{pmatrix}0\\ L^2(A_3+2A_1A_3)\\0\\ \frac{L^2}{\gamma}(A_3+2A_1A_3)\end{pmatrix}\right]$
$\tilde{Z}_{k}^{(2)}$	$\left[\begin{pmatrix}0\\ L^2(2(\lvert\bar{a}_3\rvert\lvert w_3\rvert\lvert v_1\rvert)_{k+1}^M+2(\lvert\bar{a}_3\rvert\lvert w_1\rvert\lvert v_3\rvert)_{k+1}^M+2(\lvert\bar{a}_1\rvert\lvert w_3\rvert\lvert v_1\rvert)_{k+1}^M)\\0\\ \frac{L^2}{\gamma}\left[2(\lvert\bar{a}_3\rvert\lvert w_3\rvert\lvert v_1\rvert)_{k+1}^M+2(\lvert\bar{a}_3\rvert\lvert w_1\rvert\lvert v_3\rvert)_{k+1}^M+2(\lvert\bar{a}_1\rvert\lvert w_3\rvert\lvert v_1\rvert)_{k+1}^M\right]\end{pmatrix}+2\varepsilon_{k+1}^{(3)}\begin{pmatrix}0\\ L^2(4A_3+2A_1)\\0\\ \frac{L^2}{\gamma}(4A_3+2A_1)\end{pmatrix}\right.$ $\left.+\begin{pmatrix}0\\ L^2(2(\lvert\bar{a}_3\rvert\lvert w_3\rvert\lvert v_1\rvert)_{k-1}^M+2(\lvert\bar{a}_3\rvert\lvert w_1\rvert\lvert v_3\rvert)_{k-1}^M+2(\lvert\bar{a}_1\rvert\lvert w_3\rvert\lvert v_1\rvert)_{k-1}^M)\\0\\ \frac{L^2}{\gamma}\left[2(\lvert\bar{a}_3\rvert\lvert w_3\rvert\lvert v_1\rvert)_{k-1}^M+2(\lvert\bar{a}_3\rvert\lvert w_1\rvert\lvert v_3\rvert)_{k-1}^M+2(\lvert\bar{a}_1\rvert\lvert w_3\rvert\lvert v_1\rvert)_{k-1}^M\right]\end{pmatrix}+2\varepsilon_{k-1}^{(3)}\begin{pmatrix}0\\ L^2(4A_3+2A_1)\\0\\ \frac{L^2}{\gamma}(4A_3+2A_1)\end{pmatrix}\right]$
$\tilde{Z}_{k}^{(3)}$	$\left[\begin{pmatrix}0\\ L^2((\lvert w_3\rvert^2\lvert v_3\rvert)_{k+1}^M+2(\lvert w_1\rvert\lvert w_3\rvert\lvert v_3\rvert)_{k+1}^M)\\0\\ \frac{L^2}{\gamma}\left[(\lvert w_3\rvert^2\lvert v_3\rvert)_{k+1}^M+2(\lvert w_1\rvert\lvert w_3\rvert\lvert v_3\rvert)_{k+1}^M\right]\end{pmatrix}+9\varepsilon_{k+1}^{(3)}\begin{pmatrix}0\\ L^2\\0\\ \frac{L^2}{\gamma}\end{pmatrix}+\begin{pmatrix}0\\ L^2((\lvert w_3\rvert^2\lvert v_3\rvert)_{k-1}^M+2(\lvert w_1\rvert\lvert w_3\rvert\lvert v_3\rvert)_{k-1}^M)\\0\\ \frac{L^2}{\gamma}\left[(\lvert w_3\rvert^2\lvert v_3\rvert)_{k-1}^M+2(\lvert w_1\rvert\lvert w_3\rvert\lvert v_3\rvert)_{k-1}^M\right]\end{pmatrix}+$ $\left.9\varepsilon_{k-1}^{(3)}\begin{pmatrix}0\\ L^2\\0\\ \frac{L^2}{\gamma}\end{pmatrix}\right]$
	$m\le k\le M-1$
$\tilde{Z}_{k}^{(1)}$	$\left[\frac{1}{\omega_{k+1}^s}\begin{pmatrix}1\\ L^2\lambda\\1\\ \frac{L^2}{\gamma}\end{pmatrix}+\begin{pmatrix}0\\ L^2((\lvert\bar{a}_3\rvert^2\lvert v_1\rvert)_{k+1}^M+2(\lvert\bar{a}_1\rvert\lvert\bar{a}_3\rvert\lvert v_3\rvert)_{k+1}^M)\\0\\ \frac{L^2}{\gamma}\left[(\lvert\bar{a}_3\rvert^2\lvert v_1\rvert)_{k+1}^M+2(\lvert\bar{a}_1\rvert\lvert\bar{a}_3\rvert\lvert v_3\rvert)_{k+1}^M\right]\end{pmatrix}+\varepsilon_{k+1}^{(3)}\begin{pmatrix}0\\ L^2(A_3+2A_1A_3)\\0\\ \frac{L^2}{\gamma}(A_3+2A_1A_3)\end{pmatrix}\right.$ $\left.+\frac{1}{\omega_{k-1}^s}\begin{pmatrix}1\\ L^2\lambda\\1\\ \frac{L^2}{\gamma}\end{pmatrix}+\begin{pmatrix}0\\ L^2((\lvert\bar{a}_3\rvert^2\lvert v_1\rvert)_{k-1}^M+2(\lvert\bar{a}_1\rvert\lvert\bar{a}_3\rvert\lvert v_3\rvert)_{k-1}^M)\\0\\ \frac{L^2}{\gamma}\left[(\lvert\bar{a}_3\rvert^2\lvert v_1\rvert)_{k-1}^M+2(\lvert\bar{a}_1\rvert\lvert\bar{a}_3\rvert\lvert v_3\rvert)_{k-1}^M\right]\end{pmatrix}+\varepsilon_{k-1}^{(3)}\begin{pmatrix}0\\ L^2(A_3+2A_1A_3)\\0\\ \frac{L^2}{\gamma}(A_3+2A_1A_3)\end{pmatrix}\right]$
$\tilde{Z}_{k}^{(2)}$	$\left[\begin{pmatrix}0\\ L^2(2(\lvert\bar{a}_3\rvert\lvert w_3\rvert\lvert v_1\rvert)_{k+1}^M+2(\lvert\bar{a}_3\rvert\lvert w_1\rvert\lvert v_3\rvert)_{k+1}^M+2(\lvert\bar{a}_1\rvert\lvert w_3\rvert\lvert v_1\rvert)_{k+1}^M)\\0\\ \frac{L^2}{\gamma}\left[2(\lvert\bar{a}_3\rvert\lvert w_3\rvert\lvert v_1\rvert)_{k+1}^M+2(\lvert\bar{a}_3\rvert\lvert w_1\rvert\lvert v_3\rvert)_{k+1}^M+2(\lvert\bar{a}_1\rvert\lvert w_3\rvert\lvert v_1\rvert)_{k+1}^M\right]\end{pmatrix}+2\varepsilon_{k+1}^{(3)}\begin{pmatrix}0\\ L^2(4A_3+2A_1)\\0\\ \frac{L^2}{\gamma}(4A_3+2A_1)\end{pmatrix}\right.$ $\left.+\begin{pmatrix}0\\ L^2(2(\lvert\bar{a}_3\rvert\lvert w_3\rvert\lvert v_1\rvert)_{k-1}^M+2(\lvert\bar{a}_3\rvert\lvert w_1\rvert\lvert v_3\rvert)_{k-1}^M+2(\lvert\bar{a}_1\rvert\lvert w_3\rvert\lvert v_1\rvert)_{k-1}^M)\\0\\ \frac{L^2}{\gamma}\left[2(\lvert\bar{a}_3\rvert\lvert w_3\rvert\lvert v_1\rvert)_{k-1}^M+2(\lvert\bar{a}_3\rvert\lvert w_1\rvert\lvert v_3\rvert)_{k-1}^M+2(\lvert\bar{a}_1\rvert\lvert w_3\rvert\lvert v_1\rvert)_{k-1}^M\right]\end{pmatrix}+2\varepsilon_{k-1}^{(3)}\begin{pmatrix}0\\ L^2(4A_3+2A_1)\\0\\ \frac{L^2}{\gamma}(4A_3+2A_1)\end{pmatrix}\right]$
$\tilde{Z}_{k}^{(3)}$	$\left[\begin{pmatrix}0\\ L^2((\lvert w_3\rvert^2\lvert v_3\rvert)_{k+1}^M+2(\lvert w_1\rvert\lvert w_3\rvert\lvert v_3\rvert)_{k+1}^M)\\0\\ \frac{L^2}{\gamma}\left[(\lvert w_3\rvert^2\lvert v_3\rvert)_{k+1}^M+2(\lvert w_1\rvert\lvert w_3\rvert\lvert v_3\rvert)_{k+1}^M\right]\end{pmatrix}+9\varepsilon_{k+1}^{(3)}\begin{pmatrix}0\\ L^2\\0\\ \frac{L^2}{\gamma}\end{pmatrix}+\begin{pmatrix}0\\ L^2((\lvert w_3\rvert^2\lvert v_3\rvert)_{k-1}^M+2(\lvert w_1\rvert\lvert w_3\rvert\lvert v_3\rvert)_{k-1}^M)\\0\\ \frac{L^2}{\gamma}\left[(\lvert w_3\rvert^2\lvert v_3\rvert)_{k-1}^M+2(\lvert w_1\rvert\lvert w_3\rvert\lvert v_3\rvert)_{k}^M\right]\end{pmatrix}+$ $\left.9\varepsilon_{k-1}^{(3)}\begin{pmatrix}0\\ L^2\\0\\ \frac{L^2}{\gamma}\end{pmatrix}\right]$
	$k=M$
$\tilde{Z}_{M}^{(1)}$	$(1+(\frac{M}{M-1})^s)\left[\begin{pmatrix}1\\ L^2\lambda\\1\\ \frac{L^2}{\gamma}\end{pmatrix}+\begin{pmatrix}0\\ L^2(\Sigma_{33}^{M-1}+2\Sigma_{13}^{M-1})\\0\\ \frac{L^2}{\gamma}(\Sigma_{33}^{M-1}+2\Sigma_{13}^{M-1})\end{pmatrix}\right]$
$\tilde{Z}_{M}^{(2)}$	$(1+(\frac{M}{M-1})^s)\alpha_{M-1}^{(3)}\begin{pmatrix}0\\ L^2(4A_3+2A_1)\\0\\ \frac{L^2}{\gamma}(4A_3+2A_1)\end{pmatrix}$
$\tilde{Z}_{M}^{(3)}$	$(1+(\frac{M}{M-1})^s)3\alpha_{M-1}^{(3)}\begin{pmatrix}0\\ L^2\\0\\ \frac{L^2}{\gamma}\end{pmatrix}$

Table A.1: Formulas for $\tilde{Z}_k^{(l)}$, $k=1,\dots,M$ and $l=1,2,3$.